Polymer Testing 142 (2025) 108658

Contents lists available at ScienceDirect

Polymer Testing

journal homepage: www.elsevier.com/locate/polytest

Molecular mobility and dielectric properties of dendronized side chain liquid crystalline polyamines with benzoate groups as lateral spacers

Xavier Montané [a,*], Robert Graf [b], Borja Pascual-José [c], Roberto Teruel-Juanes [c], Jordi Guardià [a], Marta Giamberini [d], José Antonio Reina [a], Amparo Ribes-Greus [c]

[a] Universitat Rovira i Virgili, Department of Analytical Chemistry and Organic Chemistry, C/Marcel·lí Domingo 1, 43007, Tarragona, Spain
[b] Max Planck Institute for Polymer Research, Ackermannweg 10, Postfach 3148, 55021, Mainz, Germany
[c] Institute of Technology of Materials (ITM), Universitat Politècnica de València (UPV), Camí de Vera s/n, 46022, Valencia, Spain
[d] Universitat Rovira i Virgili, Department of Chemical Engineering, Av. Països Catalans 26, 43007, Tarragona, Spain

ARTICLE INFO

Keywords:
Side chain liquid crystalline polyamines
Benzoate spacers
Columnar mesophases
Biomimetic membranes
Dynamic molecular mobility
Dielectric relaxation spectra

ABSTRACT

Dendronized polymers are suitable candidates for the preparation of biomimetic membranes for ion transport in fuel cells, which is nowadays a sustainable way of producing electrical energy. To prepare materials for these high-technology applications, it is necessary to understand the role of the different parts that make up these supramolecular structures. Another key factor is optimizing the preparation processes to ensure the materials achieve their maximum performance potential. Following these premises, in this work we report on the characterization of side chain liquid crystalline polyamines synthesized by chemical modification of poly[2-(aziridin-1-yl)ethanol] (PAZE) with lateral benzoate groups and the dendron 3,4,5-tris[4-(n-dodecan-1-yloxy)benzyloxy] benzoate (TAP) by using the following techniques: liquid and solid-state Nuclear Magnetic Resonance (NMR), Differential Scanning Calorimetry (DSC), Polarized Optical Microscopy (POM) and Dielectric Thermal Analysis (DETA). This in-depth investigation allowed us to understand the effect of parameters that could influence the organization of the different parts of the resulting supramolecular structures and their dynamics: introduction of benzoate lateral spacers, grafting with different amounts of TAP mesogenic group, and the thermal treatment used in the orientation of the polymer chains. NMR investigations confirmed that the melting of both copolyamines took place thanks to the mobility gained by the aliphatic tails of the TAP dendron between 256 and 272 K. Furthermore, the evaluation of variable temperature ^{13}C solid-state NMR experiments proved that the clearing transition was related to the aromatic moieties of these polyamines. DETA studies of oriented and non-oriented membranes corroborated that the application of the thermal treatment increased the temperatures of the detected transitions: γ-relaxation, α_{Tg} and α_{Clear}. The results obtained demonstrated that the adjustment of the aforementioned parameters is essential for designing membranes intended for ion transport applications.

1. Introduction

Currently, the increase of extreme events (heat waves, floods, forest fires, crop losses, etc.) and their high impact across the planet are clear evidence of the acceleration of the climate crisis [1–3]. To prevent this scenario from becoming irreversible, there is a need to reduce our carbon footprint. Among the main actions to avoid climate change is the production and use of energy from renewable sources such as fuel cells or artificial photosynthesis [4,5]. In both energy systems, polymer membranes play an important role as they separate the compartments of the fuel and the oxidant and drive the protons in a selective manner across the membrane from anode to cathode [6,7]. Although most of these membranes are still manufactured from perfluorinated polymers, their limitations (high production cost and high methanol crossover towards the polymer membrane) push investigation in this topic towards other polymers [5,8].

One of the most attractive polymers are liquid crystalline polymers (LCPs), since they combine the properties of polymers such as high thermal resistance, good mechanical strength and lightweight with the exceptional optical and electrical properties of liquid crystals [9]. This combination of properties explains why LCPs are used in distinct fields: optical devices [10], 4D printing [11], preparation of ultra-strong fibres

* Corresponding author.
E-mail address: xavier.montane@urv.cat (X. Montané).

https://doi.org/10.1016/j.polymertesting.2024.108658
Received 25 October 2024; Received in revised form 26 November 2024; Accepted 5 December 2024
Available online 6 December 2024

[12], food containers [13], in the automotive sector [14], sunlight sensors [15], medical diagnostics [16] and solid polymer electrolytes [5], among others. For example, polyazomethines are a family of polymeric materials that have been widely used to synthesize LCPs [17]. One type of LCPs are side chain liquid crystalline polymers (SCLCPs), which were reported for the first time by Finkelmann and co-workers [18]. During the last decades, one of the fields in which SCLCPs have greatly attracted the scientific community is the design of ion-conducting membranes by self-assembling that contain ion transport channels as occurs in biological processes such as photosynthesis [19].

Following this idea, one of the main investigations of our research group consists of the design, synthesis and characterization of SCLCPs by chemical modification of polyethers [20–22] and polyamines [23,24] with the dendron 3,4,5-tris[4-(n-dodecan-1-yloxy)benzyloxy]benzoic acid (TAP) to prepare novel proton transporting materials. The tapered shape of this mesogen governs the self-assembly process of the polymer backbones into helical structures, in which the polymer main chains can act as cation transport channels thanks to their columnar organization [25]. We have also reported another strategy based on the direct cationic ring-opening polymerization (CROP) of a dendritic 2-oxazoline monomer, 2-(3,4,5-tris(4-dodecyloxybenzyloxy)phenyl)-4,5-dihydro-1,3-oxazole) (TAPOx), to obtain a family of SCLC polyamines [26]. Moreover, self-supported membranes able to transport cations with high selectivity were prepared in the case of copolyethers [21,22,27]; on the other hand, it was observed that the family of side chain liquid crystalline copolyamines synthesized by chemical modification of poly[2-(aziridine-1-yl)ethanol] (PAZE) with different amounts of TAP tend to crystallize, limiting the mechanical properties of the resulting membranes [23]. To overcome this drawback, the introduction of another side group (benzoate groups) in addition to TAP let to the obtention of a family of SCLC polyamines that exhibited liquid crystalline mesophases over a broader temperature range, while preventing their crystallization [24]. Besides, homeotropically oriented membranes from these polyamines presented remarkable cation permeability and good selectivity [28]. Despite these membranes have been widely characterized, there is a considerable interest in understanding their structural organization, their phase behavior, and elucidating their structure-property relationship. Advanced solid-state NMR methods like fast magic angle spinning (MAS) performed at variable temperature, multidimensional analysis [29–31] or dielectric thermal analysis can provide detailed information on local molecular structure and mobility of these supramolecular structures [32–35].

In this way, the purpose of this work was to carry out a deep investigation on how different parameters, such as the introduction of benzoate units as lateral spacers, the grafting degree with dendritic TAP groups and the orientation of polymer chains using a thermal treatment, affect the molecular mobility of two SCLC polyamines based on PAZE modified with both benzoyl chloride and different amounts of TAP: PA3 and PA3.2 (Fig. 1). Furthermore, the analysis of the dielectric relaxation spectra allowed us to elucidate the function of the polyamine backbone and the amount of both side groups (benzoate and TAP) grafted on the resulting organization of the polymeric columns of these supramolecular structures, since they are important parameters in the design of efficient membranes for ion transport applications.

2. Experimental section

2.1. Materials

The starting polyamine (poly[2-(aziridine-1-yl)ethanol]), PAZE, was synthesized as described in a previous paper (degree of polymerization = 44, as determined by SEC-MALLS) [36]. Chemical modification of PAZE was performed using a two-step synthetic route that involves first modification of PAZE with benzoyl chloride followed by modification with the dendron TAP as described in a previous study [24].

Membranes derived from dendronized polymers were prepared by immersion precipitation process (Scheme 1a). This process consists of the following steps: 1) A homogeneous polymer solution in tetrahydrofuran (THF, 30 % w/w) was cast on a FEP (fluorinated ethylene propylene) sheet support and immersed in a bath of Milli-Q water; 2) The solvent diffused into the precipitation bath, while the non-solvent (water) diffused into the cast film; 3) After a time, in which the solvent and the non-solvent were exchanged, the polymer solution (wet film) became thermodynamically unstable and demixing took place; 4) Afterward, a solid polymer membrane was formed with an asymmetric structure; 5) Finally, the membrane was dried overnight at room temperature (RT = 25 ± 5 °C).

Oriented membranes were obtained by using a baking process (Scheme 1b). In this thermal process, the polymer membrane along with FEP sheet was mounted on a Linkam TP92 (Linkam Scientific Instruments, Tadworth, UK) hot stage and it was heated above the clearing temperature (130 °C in the case of the tested membranes); then it was allowed to cool slowly (0.5 °C/min) to a temperature slightly below than the clearing temperature of the polyamine (this temperature was chosen accordingly to the clearing temperature of each LC copolymer). At this temperature, an annealing process was applied during 24 h to allow the orientation of the polymer chains into columns, which was followed by slow cooling (0.5 °C/min) to 30 °C. After the baking process, the membrane was kept at RT for approximately 1 h and then it was separated from the FEP sheet and obtained as an intact, uniform membrane with thickness between 120 and 200 μm. The thickness of the membranes was measured using a micrometer with a sensitivity of 2 μm. The

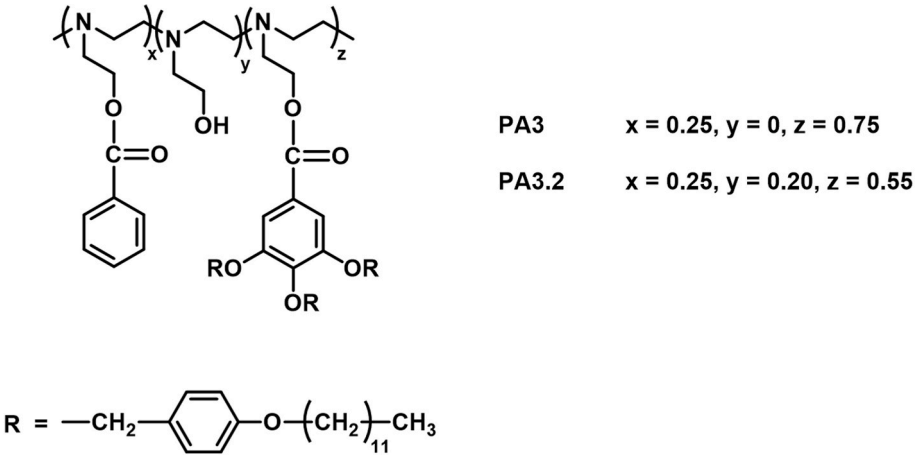

Fig. 1. Chemical structures and modification degrees of PA3 and PA3.2 copolyamines.

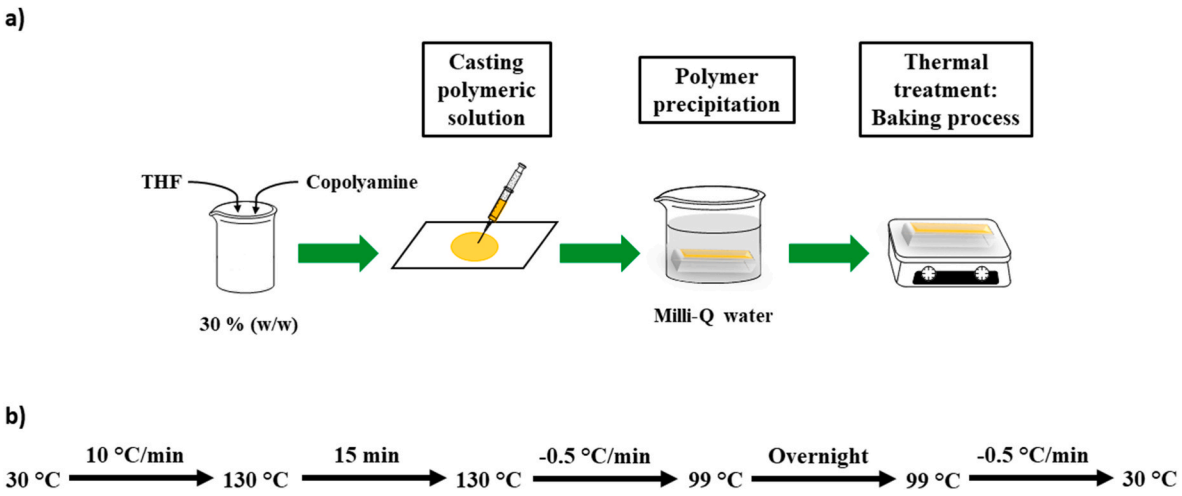

Scheme 1. a) Immersion precipitation process used for the preparation of self-supported polyamine-based membranes. b) Thermal treatment (or baking process) applied to orient membranes prepared with copolyamines PA3 and PA3.2.

measurements were carried out at various points, and the membranes were found to have constant thickness. Oriented membranes are labelled with the suffix: O.

2.2. Characterization techniques

2.2.1. Differential scanning calorimetry (DSC)

Calorimetric analyses were carried out on a Mettler DSC-821 instruments calibrated using indium (156.6 °C) and zinc (419.6 °C) pearls. Samples were placed in an aluminium standard crucible of 40 μL with pierced lids (between 4 and 6 mg of sample), which were analysed in N_2 atmosphere (gas flow rate of 50 cm^3/min). Heating and cooling rate of 10 °C/min was always employed.

2.2.2. Polarized optical microscopy (POM)

Liquid crystal mesophases were investigated by polarized optical microscopy (POM). The textures of the samples were observed with an Axiolab Zeiss optical microscope equipped with a Linkam TP92 hot stage and a Moticam S6 digital camera.

2.2.3. Solution-state nuclear magnetic resonance (NMR) spectroscopy

^{1}H NMR and ^{13}C NMR spectra were recorded at 400 and 100.4 MHz, respectively, on a Varian Gemini 400 spectrometer with proton noise decoupling for ^{13}C NMR. The central peak of the solvent was taken as the reference, and the chemical shifts were given in parts per million from TMS (tetramethylsilane). The ^{13}C NMR spectra of the polymers were recorded at 303.2 K, with a flip angle of 45°, and the number of transients ranged from 20,000 to 40,000 with 10–20 % (w/v) sample solutions in deuterated chloroform ($CDCl_3$). A pulse delay time of 5 s for the ^{1}H NMR spectrum was used.

Quantitative ^{13}C NMR spectra were performed using deuterated chloroform ($CDCl_3$) at 30 °C with a pulse delay time of 5 s. Delay time was selected on the basis of the relaxation times determined for the monomer 1-(2-hydroxyethyl)aziridine.

2.2.4. Solid-state nuclear magnetic resonance (NMR) spectroscopy

Solid-state NMR experiments were performed using a Bruker Avance III NMR spectrometer (Bruker, Billerica, MA, USA) equipped with a superconducting magnet: 19.9 T standard bore (850.27 MHz ^{1}H Larmor frequency and 213.8 MHz for ^{13}C). Commercial double resonance MAS probes supporting zirconia rotors with 2.5 mm and 4.0 mm outer diameter allowed the experiments to be performed at MAS spinning frequencies of 25 and 10 kHz, respectively. The 90° pulse length used was 2.5 μs and the repetition delay 2 s. The cross-polarisation magic angle spinning (CP-MAS) spectra have been acquired with a CP contact pulse length of 1 ms and 2048 transients, using SPINAL64 decoupling during acquisition. The temperature was varied in eight linearly spaced steps in the range 256–364 K using a BSVT temperature control and a BCU-II cooling unit. The spectra were externally referenced to the CH_3-signal of solid L-Alanine (1.34 ppm for ^{1}H and 20.5 ppm for ^{13}C).

The experiments listed below were performed.

- ^{1}H MAS (Magic angle spinning) and ^{13}C CP-MAS (cross-polarisation magic angle spinning) variable temperature (VT) studies.
- ^{13}C INEPT (Insensitive Nuclei Enhanced by Polarisation Transfer Experiment) MAS, which in our case was: ^{1}H → ^{13}C transfer, using a 145 Hz J coupling.

2.2.5. Dielectric thermal analysis (DETA)

The impedance measurements were conducted using a Novocontrol Broadband Dielectric Impedance Spectrometer (BDIS) connected to a Novocontrol Alfa-A Frequency Response Analyzer. The measurements were run at a frequency of 10^3 Hz between 130 and 390 K. All the measurements were performed under isothermal conditions by increasing steps by 2.5 K.

The dielectric spectra were analysed in terms of the complex permittivity (ε*). All the characteristic parameters of each relaxation process were determined as shown in the following equation:

$$\varepsilon^*(\omega) = \varepsilon_\infty + \frac{\Delta\varepsilon}{(1 + (i\omega\tau_{HN})^\alpha)^\beta} \quad (1)$$

In this equation, τ_{HN} is the Havriliak-Negami relaxation time, α and β are parameters corresponding to the width and asymmetry of the relaxation peak, respectively. Δε is the value of the relaxation strength.

3. Results and discussion

Polyamines bearing benzoate and the tapered 3,4,5-tris[4-(n-dodecan-1-yloxy)benzyloxy]benzoic acid (TAP) dendron were synthesized by chemical modification of poly[2-(aziridine-1-yl)ethanol] (PAZE) as described in a previous work by following a two-step pathway [24]. The resulting degrees of modification of the copolyamines characterized in this paper are visualized in Fig. 1. The modification degrees were calculated based on solution NMR spectroscopy data. Table 1 reports ^{1}H and ^{13}C NMR solution spectrum data of PA3.2 performed at RT in $CDCl_3$ (Figure S1 and Figure S2). Quantification was carried out from the ^{13}C NMR by comparing the areas of the carbon of methylene c and c'' in the modified monomeric units (signal between 62.6 and 63.0 ppm)

Table 1
NMR data and structure of the PA3.2 copolymer in $CDCl_3$.

^{1}H NMR		^{13}C NMR	
Signal (ppm)	Assignment	Signal (ppm)	Assignment
12	0.8	**12**	14.2
3–11	1.1–1.4	**11**	22.8
2	1.6	**3**	26.2
a, a', a'', b, b', b''	2.3–3.0	**2, 4–9**	29.5–29.8
c'	3.5	**10**	32.0
1	3.8	**a, a', a'', b, b', b''**	51.4–56.8
c, c''	4.3	**c'**	60.1
e''	4.8	**c, c''**	62.6–63.0
Ar	6.5–7.9	**1**	68.0
		e' lateral	71.0
		e'' central	74.8
		II'	108.9
		VII'	114.0–114.5
		I'	125.1
		I-IV, V', VI'	128.6–133.0
		IV'	142.7
		III'	152.7
		VIII'	159.0
		COO	166.1–166.4

and the carbon of methylene c' in the unmodified monomeric unit (signal at 60.1 ppm).

3.1. Calorimetric characterization and evaluation of the molecular mobility

The two synthesized polyamines exhibited a LC mesophase. The DSC analysis (Fig. S3) of these copolymers put into evidence two endotherms: the first was assigned to the melting phenomenon and the second one to the clearing transition, respectively, by the aid of POM. The growth of the LC textures on cooling from isotropization was observed by POM (Fig. 2). Table 2 summarizes the values of the transitions observed for PA3 and PA3.2. As observed, both copolymers melt at similar temperatures. Regarding their clearing temperatures and enthalpies, they increased on increasing the content of the mesogenic group, similarly to what was reported for columnar copolyethers and copolyamines modified only with TAP [21,23]. On the other hand, T_g was not observed in any of these two copolymers by DSC.

Furthermore, VT ^{1}H MAS and ^{13}C CP-MAS NMR experiments were carried out to understand the nature of dynamic processes that occur in these copolyamines.

Fig. 3 shows the ^{1}H MAS and ^{13}C CP-MAS NMR spectra of copolyamine PA3 at variable temperature. As observed in the ^{1}H MAS NMR spectra (Fig. 3a), this copolyamine is very rigid at 256 K. Nevertheless, the proton spectra exhibit a remarkable line narrowing with the increasing temperature between 256 and 364 K. The differences in the definition of the peaks in the spectra recorded at 256 and 272 K proved that the copolymer becomes more mobile after surpassing its melting temperature (260 K). In particular, the best spectral resolution corresponds to the outer aliphatic side chains of the TAP dendron (0.7–1.7 ppm) since two different peaks can be observed in the spectra recorded at 272 K. Moreover, two new weak peaks can be detected in the spectra when it is recorded at 364 K, that is.

- A peak centred at 7.6 ppm, which is attributed to the protons in *orto*-position of the benzoate units attached to the copolymer.
- Another peak centred at 4.4 ppm that corresponds to the methylene units of the copolyamine main chain.

The observation of these two peaks in the ^{1}H MAS spectra indicates that both the external and internal parts of the polymer columnar structures are quite mobile, and that the system is close to the clearing temperature detected by DSC and POM (373–377 K).

In the ^{13}C CP-MAS NMR spectra, a homogeneous decay in intensity of the peaks attributed to the side chains and the polymer backbone is observed between 256 and 364 K, which implies that the molecular mobility of the polymer chains increases (Fig. 3b).

In a similar manner as described for ^{1}H MAS NMR, the peaks in the ^{13}C CP-MAS NMR spectrum at 256 K are very broad when compared with the peaks of the same spectrum performed at 272 K. In the aliphatic region, the intensity of the signal centred at 14.7 ppm, which corresponds to the methyl group of the aliphatic chains of the side dendrons, decrease at higher temperature than the melting point (260 K), thus proving that the outer part of the dendrons gain some mobility in this temperature range. As observed in Fig. 3b, a broad peak centred at 31.6 ppm in the spectrum recorded at 256 K is attributed to the carbons 2 and 4–9 of the TAP chains being in all-*anti* conformation. When the temperature is increased to 272 K, this signal is split into two narrower signals and one of them moves upfield in the spectrum (around 31.0 ppm); this can be associated to conformational changes of the aliphatic chains of TAP groups from a predominant *anti* at low temperatures to a more random with stronger *gauche* contributions. This information is in agreement with the observed transition at 260 K by DSC and confirms that the outer aliphatic regions of the dendrons contribute to the melting of PA3 copolymer.

The signals attributed to the main chain of the polymer can be observed as a broad peak in the region between 42.7 and 64.9 ppm when the ^{13}C CP-MAS spectra is recorded at low temperatures (Fig. 3c). At 256 K, the attached benzoate and TAP groups induce stiffness of the inner part of the polymer and an irregular conformation of virgin samples (Fig. 4). As a result, this irregular conformation determines a very broad distribution of the signals attributed to the carbons of the polymer main chain (signals a, a' and a'') and the lateral ethylidene groups bonded to the nitrogen atoms of the polyamine backbone (signals b, b',

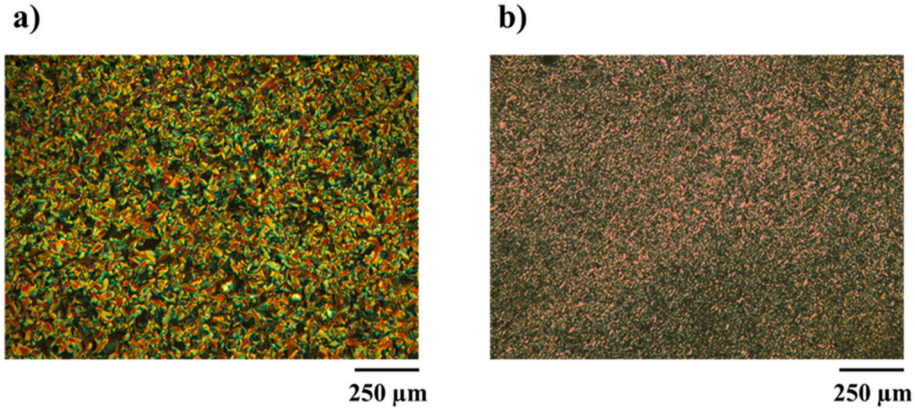

Fig. 2. Optical micrographs between crossed polars recorded on cooling from the isotropic phase of: a) PA3 at 348 K, and b) PA3.2 at 343 K.

Table 2
Transitions observed by DSC, ^{1}H MAS and ^{13}C CP-MAS NMR for PA3 and PA3.2 copolyamines and associated clearing enthalpy as determined by DSC.

Copolyamine	Transition	*DSC (K)* [a]	*ΔH_c (kJ/mol)* [b]	*^{1}H and ^{13}C CP-MAS NMR (K)* [c]	*Chemical shifts (ppm) of ^{1}H MAS NMR* [d]	Chemical shifts (ppm) of ^{13}C CP-MAS NMR [d]
PA3	Melting	260[e]	–	256–272	0.0–8.5	14.7–166.6
	Clearing	373–377	1.7	Not reached[f]	–	–
PA3.2	Melting	263[e]	–	256–272	0.0–8.5	14.7–166.2
	Clearing	366–370	1.4	348–364	0.7–1.6; 3.0–4.9; 5.8–7.8	22.9; 26.4–32.5; 67.8; 71.1; 74.7; 114.1; 129.9 (peaks that vanish)

[a] Determined by DSC second heating scan and POM [24].
[b] Associated enthalpy to the clearing transition expressed per mol of TAP group as determined by DSC second heating scan [24].
[c] Temperature at which melting and clearing transitions are detected.
[d] Chemical shifts of the groups involved in the melting and clearing transitions.
[e] Temperature of the peak maximum of the melting endotherm.
[f] Clearing temperature not reached using the selected VT range.

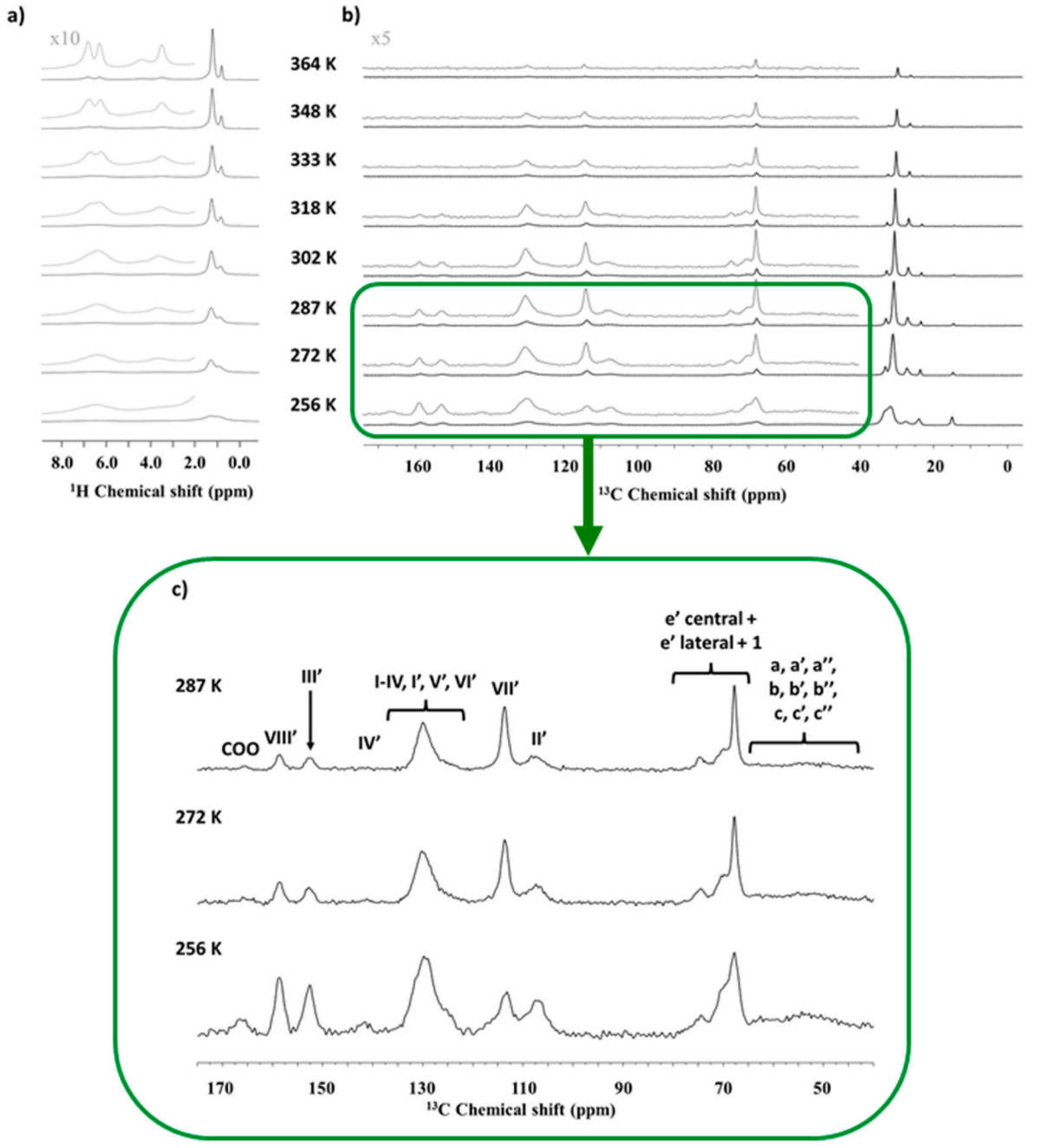

Fig. 3. a) ^{1}H MAS NMR, b) ^{13}C CP-MAS NMR spectra of copolyamine PA3 at VT, and c) zoom of the ^{13}C CP-MAS NMR spectra of copolyamine PA3 at VT (256–287 K). The given temperature values are corrected for the frictional heating under fast MAS conditions.

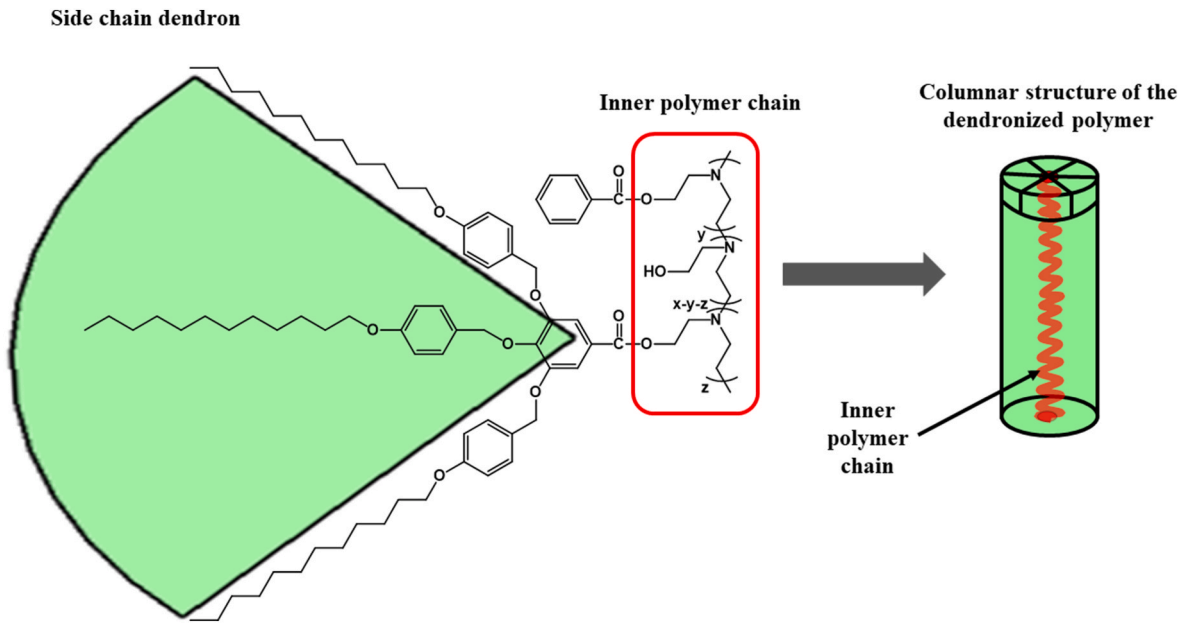

Fig. 4. General chemical structure of dendronized copolyamines that self-assemble into columnar structures.

b'', c, c' and c'') in the ^{13}C CP-MAS spectra at lower temperatures than the melting. The intensity of this broad signal decreases considerably when the temperature rises, which shows that the polymer main chain also gains some mobility above the melting point, as reasonably expected.

Furthermore, the presence of some residual peaks in the spectrum acquired at 364 K (Fig. 3b) indicates that the clearing temperature of this copolymer was not reached under the employed conditions; nevertheless, their low intensity proves that this temperature is close to the clearing transition. For this SCLC polyamine, the peaks observed in the aliphatic (26.2–31.9 and 67.8 ppm) and the aromatic regions (114.1 and 129.5 ppm) at the spectrum recorded at 364 K corroborate that the aromatic moieties and their adjacent aliphatic regions are mainly involved in the clearing of PA3.

To compare the behaviour of both materials, copolyamine PA3.2 was also investigated using the VT ^{1}H MAS and ^{13}C-CP-MAS NMR experiments. Table 2 summarizes the transitions observed by DSC, ^{1}H MAS and ^{13}C CP-MAS NMR analyses for this copolyamine and the associated enthalpy to the clearing as determined by DSC.

Both ^{1}H MAS and ^{13}C CP-MAS NMR spectra of copolyamine PA3.2 at VT are displayed in Fig. 5. From ^{1}H MAS spectra (Fig. 5a), PA3.2 presents a rigid structure at 256 K, analogously to copolyamine PA3. At 272 K the peak corresponding to the aliphatic chains of the dendron (region between 0.5 and 2 ppm) was split into 2 peaks, thus showing that the outer part of the columnar structures had acquired some mobility after melting (at 266 K, as from DSC analysis). Moreover, proton spectra exhibit a gradual line narrowing on increasing the temperature between 256 and 364 K. The main difference between copolyamines PA3 and PA3.2 is that the peaks attributed to the protons in *orto*-position of the benzoate units attached to the copolymer (7.7 ppm) and the ones that correspond to the methylene units of the main chain (centred at 4.5 ppm) can be observed when the spectra was recorded at 348 K for the

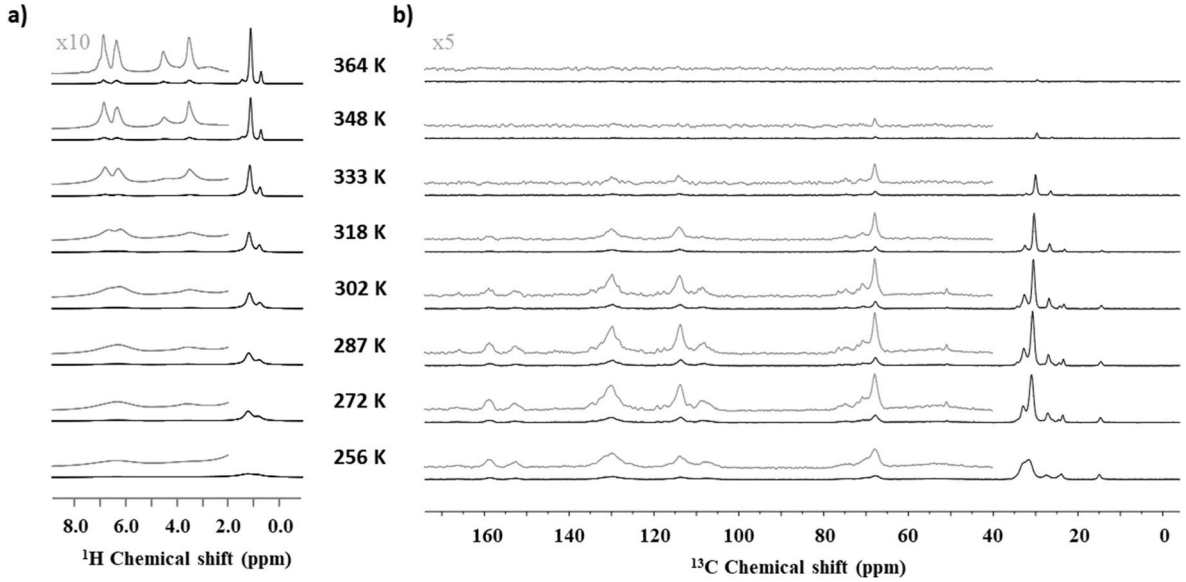

Fig. 5. a) ^{1}H MAS NMR, and b) ^{13}C CP-MAS NMR spectra of copolyamine PA3.2 at VT. The given temperature values are corrected for the frictional heating under fast MAS conditions.

sample PA3.2, which does not happen for copolyamine PA3. This is in agreement with the slightly lower clearing temperature of copolyamine PA3.2 as detected by DSC and POM (366–370 K). In the case of PA3, these peaks were only detected from 364 K, which reveals that this macromolecule requires more energy for these parts to have certain mobility.

Regarding the ^{13}C CP-MAS NMR spectra, the peaks are very broad at temperatures below the melting. Once it is surpassed, a uniform drop in intensity of the spectrum line is observed as the temperature was increased. From what is observed in Fig. 5b, the clearing of this copolymer takes place between 348 and 364 K because all the peaks have almost vanished at the spectrum performed at 364 K (only a tiny signal of the methylene units related to the aliphatic chain of TAP is still observable).

As for the PA3.2 copolymer, the following changes were also seen for this sample.

- The decrease in intensity corresponding to the signal attributed to the -CH_3 group of the aliphatic chains of the side dendron (at 14.7 ppm) at temperatures above the melting point.
- In the same temperature ranges, the changes associated to the different chemical shift and the shape of the peak attributed to the vast majority of the carbons of the aliphatic chain of TAP revealed that these side chains become mobile above the melting. As an example, the broad signal centred at 31.7 ppm in the spectrum recorded at 256 K, which is attributed to the carbons 2 and 4–9 of Table 1 in all-*anti* conformation, splits in two thin peaks in the spectrum recorded at 272 K, demonstrating that the predominant *anti* conformation has changed to a mainly *gauche* conformation.
- Furthermore, the intensity of the broad peak attributed to the carbons of the polymer main chain (between 45.0 and 64.1 ppm in Fig. S4) suffers a considerable drop when the melting temperature is surpassed (as observed in the ^{13}C CP-MAS NMR spectra recorded at 272 and 287 K, respectively).

To support these findings, a complementary experiment that allows the observation of the mobile regions (VT ^{13}C INEPT MAS NMR) was carried out. The resulting spectra are presented in Fig. 6. As observed in the spectra, only the aliphatic chains of the dendron gain some mobility between 333 and 348 K since peaks corresponding to the aliphatic region mostly appear in the spectra recorded at both temperatures. Moreover, most of the carbons of the side alkyl chains are quite mobile (carbons 2–12), while carbons C1, and some aromatic carbons also present a certain mobility at this temperature range. It is evident that the intensity of the peak that appears at 14.7 ppm, which corresponds to the methyl group of the long aliphatic chains of TAP is higher than the other peaks at these temperatures. This points out that the terminal -CH_3 groups are more mobile than the rest of the aliphatic chain between 333 and 348 K. This fact, combined with the gradual decrease in the intensity of the same peak observed in the ^{13}C CP-MAS spectra (Fig. 5b), confirms that the melting transition is correlated with the outer part of the dendrons. However, the signal intensities are still biased by restricted mobility at some sites. When we are around the clearing temperature (364 K), intense signals that are almost quantitative can be observed in all the regions of the spectrum (aliphatic, -OCH_2- and the aromatic regions of the copolymer structure), which suggest that all these moieties are completely mobile and that all of them are involved in the clearing transition.

In this way, the combination of different NMR techniques allowed the interpretation of the chemical structure and to elucidate the nature of the different thermal transitions previously determined by DSC of the investigated LC copolyamines. For these systems, two transitions have been detected: The first one, which is attributed to the melting and occurs between 256 and 272 K, is caused by the gain of mobility of the outer part of the TAP side dendrons. The second one, which is attributed to the clearing temperature, could only be detected for copolyamine PA3.2 in the temperature range employed by solid-state NMR. In this case, the comparison of ^{13}C CP-MAS and ^{13}C INEPT MAS NMR is useful to determine the rigid and mobile parts at temperatures below and above the clearing.

3.2. Dielectric thermal analysis (DETA) characterization

The dielectric spectrum displays the response of the molecular dipoles to an applied electric field, which, combined with the other structural information results, enhances and clarifies polymer molecular dynamics. Indeed, dielectric analysis is a well-established method that can be used to monitor the macroscopic properties of the copolymers

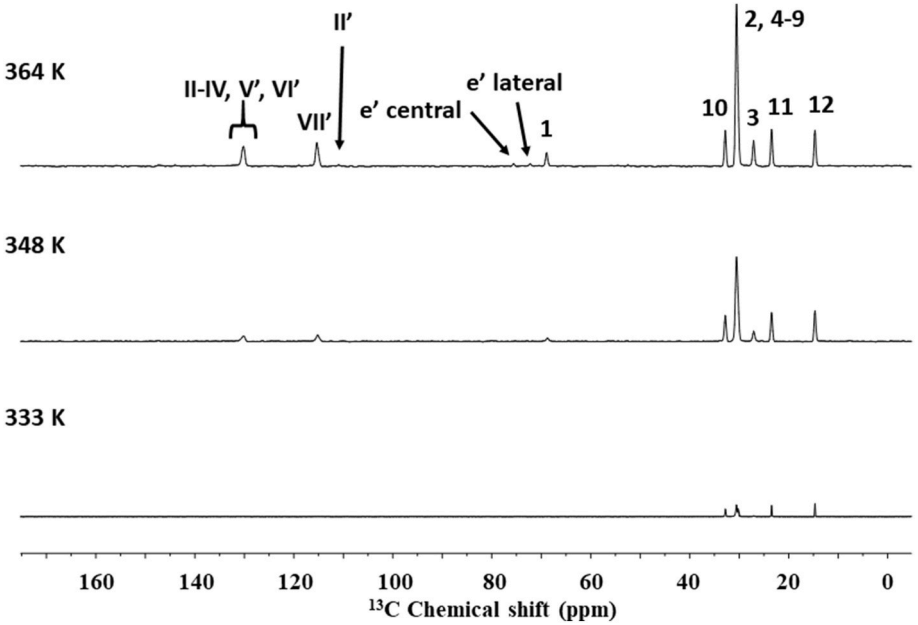

Fig. 6. a) ^{13}C INEPT MAS NMR spectra of copolyamine PA3.2 at variable temperature (333–364 K). The given temperature values are corrected for the frictional heating under fast MAS conditions.

under investigation. In this way, dielectric measurements were performed on non-oriented and oriented membranes based on PA3 and oriented membranes based on PA3.2 copolymers. Accordingly, the differences found in the molecular dynamics of each membrane depend on two factors: the concentration of the TAP dendron and the thermal treatment employed. These factors alter the copolymer free space, orientation, and crystallinity, affecting molecular motions. Furthermore, the effect of the addition of lateral benzoate groups was also investigated in order to compare it with that of the same LC polyamines modified only with the dendron TAP.

The dielectric relaxation spectra of these copolymers were measured in terms of the loss tangent (tan δ) across a wide range of temperatures to observe the melting, glass transition, and clearing processes. Some of these processes were detected using the aforementioned techniques; on the other hand, dielectric analysis allows detecting changes of molecular mobility more accurately and can confirm the presence of secondary relaxations.

The dielectric spectra of the dendronized polyamines are presented in Fig. 7, illustrating the differences in the dielectric behaviour of each of the copolymers. These dendronized polyamines are composed of three dielectric relaxations labelled as γ, α_{Tg}, and α_{Clear}, respectively, in increasing temperature order, which are associated with distinct molecular dynamics within the material.

At low temperatures, specifically around 150 K at a frequency of 10^3 Hz, the γ-relaxation is found. Due to the low temperature at which it occurs, this molecular motion has not been detected using the previous experimental techniques employed to characterise these copolymers, as has been observed with similar copolymers [33,34]. This motion is a non-cooperative movement that only depends on the benzyloxy terminal group of the dendritic mesogen. The concentration of the TAP dendron appears to have only a minor influence on the movement of this group of molecules. As expected, the side chain dendrons will likely have greater significance in the movements associated with the main chain. Nevertheless, the orientation of the PA3 derived membranes shifts the peak of the γ-relaxation to higher temperatures. This shift may be attributed to the polymer tendency to self-organize into a more constrained structure when these copolymers are subjected to annealing due to an exorecognition process of the side chain dendrons by intermolecular forces and their following self-assembly. The primary difference between oriented and non-oriented copolymers is the arrangement of their microstructures. Oriented copolymers, which have columns aligned parallel to one another, display greater macromolecular order compared to non-oriented copolymers. On the other hand, the reduction of the TAP side groups in oriented membranes (PA3.2) reduces the temperature of the γ-relaxation. This fact could be explained by the presence of some free hydroxyl groups that can contribute to the crystallinity of this copolyamine through hydrogen bonding.

At higher temperatures, α_{Tg} relaxations appear, which in other similar copolymers have been associated with the glass transition [33,34]. It should be noted that glass transition cannot be detected on the DSC thermograms (Fig. S3). However, polymer melting also takes place in this temperature range, overlapping with the glass transition temperature. This zone represents a critical thermal threshold where the molecular dynamics of the copolyamines undergo significant changes. During the glass transition, large sections of the polymer chains begin to gain mobility as the temperature reaches the transition threshold. This is confirmed by the data depicted in Fig. 3b, where it is observed that the molecular mobility of the polymer chains increases between 256 and 364 K. In Fig. 7, the α_{Tg} relaxation peak appears between 250 and 270 K at a frequency of 10^3 Hz. As described above in the ^{13}C CP-MAS NMR of both copolyamines (Figs. 3 and **5**), this is evidenced by the decrease in intensity of the signal centred at 14.7 ppm when the spectra recorded at 256 and 272 K were compared. This peak is attributed to the methyl groups of the side aliphatic chains, whose conformation also changed at this temperature range. It is important to underline that α_{Tg}-relaxation shows different behaviour depending on the copolymer substitution degree and the orientation of the membrane. α_{Tg}-relaxation of copolyamine PA3 occurs at higher temperatures when compared to copolyamine PA3.2. This result is in line with expectations, as the greater quantity of dendrons within PA3 structure determines that more thermal energy is needed to initiate molecular motions. The width of these relaxation curves remains constant, suggesting that the extent of molecular motion is comparable in both copolymers. However, the orientation has a noticeable effect on the values of α_{Tg} temperature peak, since in the case of the non-oriented membrane, this relaxation occurs at lower temperatures than its oriented counterpart. On the other hand, the non-complete lateral modification of the copolyamine PA3.2 decreases the temperature of this transition, as commented before with the γ-relaxation. α_{Tg} relaxation occurring in the amorphous regions is more prevalent in the less ordered macromolecular structures, which are predominant in non-oriented membranes, in contrast to the more ordered polymer columns present in oriented membranes. These results align with previous research on dendronized polyamines, where similar patterns of temperature dependence in relation to membrane orientation were reported [33,34]. The thermal treatment and its consequent orientation shift the dielectric spectrum towards higher temperatures, while the introduction of benzoate spacers seems not to affect these transitions too much when compared to the same polyamines only

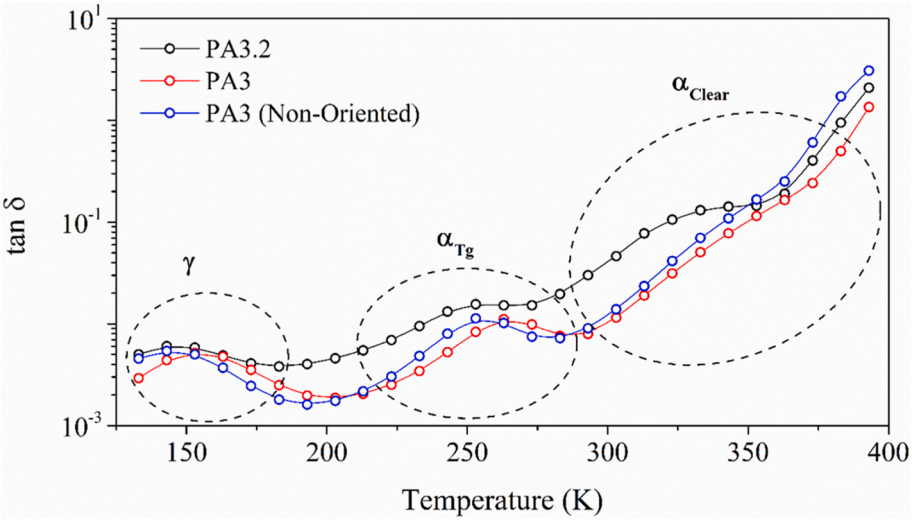

Fig. 7. Loss tangent (tan δ) of the PA3.2 and PA3 (oriented and non-oriented) at a frequency of 10^3 Hz.

modified with TAP [33]. The higher macromolecular order induced by heat treatment restricts molecular motion, resulting in a more pronounced increase in the glass transition temperature than that caused by TAP groups. These results further emphasize the influence of structural orientation on the thermal and dynamic characteristics of these copolymers.

Fig. 7 shows another transition, which is associated to the α_{Clear} relaxation. Similar to other copolymers investigated, it is related to the clearing transition [33,34]. The values of the α_{Clear} temperature peaks at a frequency of 10^3 Hz are located between 335 and 345 K for the two copolyamines studied. Regarding the α_{Clear} relaxation, it seems that the copolymer orientation does not affect it, probably because the melting process of the side chains occurs at a lower temperature than the clearing process, as proved before by DSC and POM [24]. As for this transition, the introduction of benzoate lateral spacers seems to be the most important factor as seen in the curves represented in Fig. 7. In fact, the α_{Clear} relaxation of these copolyamines is higher than that showed by side chain liquid crystalline polyamines prepared by chemical modification of PAZE with only TAP side groups [33]. Indeed, Fig. 7 confirms that the α_{Clear} relaxation is broader and occurs at lower temperatures in copolyamine PA3.2 than in copolyamine PA3. This suggests that the presence of the benzoate moieties plays a crucial role in inhibiting crystallinity and enhancing the copolymer mobility, since it introduces structural irregularities.

4. Conclusions

Molecular mobility of two side chain liquid crystalline polyamines modified with benzoate lateral spacers and with different degrees of modification with TAP dendrons was characterized by the combination of different techniques: liquid and solid-state NMR (^{1}H MAS NMR, ^{13}CP-MAS NMR and ^{13}C INEPT MAS VT studies), DSC, POM and DETA to elucidate their local structure and the nature of their different thermal transitions.

Solid-state NMR investigations confirmed that both copolymers melt between 256 and 272 K, as checked before by means of DSC. Furthermore, we proved that the methyl group at the end of the aliphatic chains of TAP mesogens gains some mobility at higher temperatures than the melting point, denoting that this transition involves mainly the outer part of the side chain dendrons grafted to the copolymer.

Concerning the clearing temperature, the introduction of lateral benzoate lateral spacers in addition to TAP mesogen provided these copolyamines with a higher clearing temperature compared to the copolyamines that were only modified with TAP, reported in previous studies. By solid-state NMR, only the clearing temperature of copolyamine PA3.2 was detected between 348 and 364 K, while the same transition for the copolyamine PA3 was not achieved with the accessible VT range. The higher degree of modification of PA3 with the dendron TAP explains why some regions of the copolymers are still rigid at the highest temperature tested. Moreover, the analysis of ^{13}C INEPT MAS NMR of copolyamine PA3.2 confirms that all parts of the copolymer are completely mobile at 364 K, which practically matches the clearing temperature detected by DSC and POM. Slightly lower clearing temperatures, although showing the same trend, were obtained when these samples were analysed by means of DETA due to the difference in the frequency of the analyses.

Moreover, the dielectric spectra of oriented and unoriented membranes derived from these copolymers show three distinct dielectric relaxations for each of them. The main dissimilarity between oriented and non-oriented membranes lies in the order of their structures at the molecular level: polymer chains in thermally treated membranes exhibit higher macromolecular order, and as a result of it, the relaxations observed in the spectrum are shifted to higher temperatures. In contrast, decreasing the degree of modification with the TAP dendron from 75 to 55 % decreases the temperature of these transitions, since the greater quantity of lateral dendrons within the structure increases the thermal energy needed for molecular motions. Thus, the incorporation of benzoate lateral groups and the modification degree with TAP influence the thermal response of these dendronized copolyamines, which exhibit liquid crystal behaviour in a temperature range above 100 °C thanks to the presence of benzoate lateral spacers.

In conclusion, the combination of solid-state NMR with dielectric thermal analysis provides useful information about the local structure of dendronized polymers, likewise about the molecular mobility in these complex structures. Additionally, these studies are fundamental to fine-tuning their function, further emphasizing the influence of structural orientation on their thermal and dynamic characteristics.

CRediT authorship contribution statement

Xavier Montané: Writing – original draft, Validation, Supervision, Resources, Methodology, Investigation, Funding acquisition, Formal analysis, Data curation, Conceptualization. **Robert Graf:** Writing – review & editing, Supervision, Methodology, Investigation, Formal analysis, Data curation, Conceptualization. **Borja Pascual-José:** Writing – original draft, Methodology, Investigation, Formal analysis. **Roberto Teruel-Juanes:** Writing – original draft, Methodology, Investigation, Formal analysis. **Jordi Guardià:** Methodology, Investigation. **Marta Giamberini:** Writing – review & editing, Validation, Supervision, Resources, Project administration, Funding acquisition, Formal analysis, Data curation, Conceptualization. **José Antonio Reina:** Writing – review & editing, Validation, Supervision, Project administration, Formal analysis, Data curation, Conceptualization. **Amparo Ribes-Greus:** Writing – review & editing, Project administration, Methodology, Funding acquisition, Formal analysis, Data curation, Conceptualization.

Data availability

The raw data required to reproduce these findings cannot be shared at this time due to technical limitations, but supplementary information will be sent on request.

Declaration of competing interest

The authors declare that they have no known competing financial interests or personal relationships that could have appeared to influence the work reported in this paper.

Acknowledgements

This work was supported by the Ministerio de Ciencia e Innovación, grant number PID2020-116322RB-C32. This project has received funding from the European Union's Horizon 2020 research and innovation programme under the Marie Skłodowska-Curie grant agreement No. 713679.

Appendix A. Supplementary data

Supplementary data to this article can be found online at https://doi.org/10.1016/j.polymertesting.2024.108658.

Data availability

Data will be made available on request.

References

[1] K. Abbass, M.Z. Qasim, H. Song, M. Murshed, H. Mahmood, I. Younis, A review of the global climate change impacts, adaptation, and sustainable mitigation measures, Environ. Sci. Pollut. Res. 29 (2022) 42539–42559, https://doi.org/10.1007/s11356-022-19718-6.

[2] F. Bibi, A. Rahman, An overview of climate change impacts on agriculture and their mitigation strategies, Agric. For. 13 (2023) 1–16, https://doi.org/10.3390/agriculture13081508.
[3] M.J. Siegert, M.J. Bentley, A. Atkinson, T.J. Bracegirdle, P. Convey, B. Davies, R. Downie, A.E. Hogg, C. Holmes, K.A. Hughes, M.P. Meredith, N. Ross, J. Rumble, J. Wilkinson, Antarctic extreme events, Front. Environ. Sci. 11 (2023) 1229283, https://doi.org/10.3389/fenvs.2023.1229283.
[4] M.E. El-Khouly, E. El-Mohsnawy, S. Fukuzumi, Solar energy conversion: from natural to artificial photosynthesis, J. Photochem. Photobiol. C Photochem. Rev. 31 (2017) 36–83, https://doi.org/10.1016/j.jphotochemrev.2017.02.001.
[5] A. Zare, X. Montané, J.A. Reina, M. Giamberini, Applications of membranes in sustainable energy systems: energy production and storage, Pol. Eng. (2022) 219–248, https://doi.org/10.1515/9783110733822-007.
[6] L. Fan, Z. Tu, S.H. Chan, Recent development of hydrogen and fuel cell technologies: a review, Energy Rep. 7 (2021) 8421–8446, https://doi.org/10.1016/j.egyr.2021.08.003.
[7] A. Javed, P. Palafox Gonzalez, V. Thangadurai, A critical review of electrolytes for advanced low- and high-temperature polymer electrolyte membrane fuel cells, ACS Appl. Mater. Interfaces 15 (2023) 29674–29699, https://doi.org/10.1021/acsami.3c02635.
[8] N.A.M. Harun, N. Shaari, N.F.H. Nik Zaiman, A review of alternative polymer electrolyte membrane for fuel cell application based on sulfonated poly(ether ether ketone), Int. J. Energy Res. 45 (2021) 19671–19708, https://doi.org/10.1002/er.7048.
[9] X. Lyu, A. Xiao, D. Shi, Y. Li, Z. Shen, E.Q. Chen, S. Zheng, X.H. Fan, Q.F. Zhou, Liquid crystalline polymers: discovery, development, and the future, Polymer 202 (2020) 122740, https://doi.org/10.1016/j.polymer.2020.122740.
[10] S.J.D. Lugger, S.J.A. Houben, Y. Foelen, M.G. Debije, A.P.H.J. Schenning, D. J. Mulder, Hydrogen-bonded supramolecular liquid crystal polymers: smart materials with stimuli-responsive, self-healing, and recyclable properties, Chem. Rev. 122 (2022) 4946–4975, https://doi.org/10.1021/acs.chemrev.1c00330.
[11] A. Akram, T.G. Shahzady, S. Hussain, N.A. Saad, M.T. Islam, M. Ikram, Liquid crystal polymers: overview of characteristics and applications in communication and biomedical technologies, Russ. J. Appl. Chem. 94 (2021) 1585–1593, https://doi.org/10.1134/S107042722112003X.
[12] X. Hu, Z. Xu, Z. Liu, C. Gao, Liquid crystal self-templating approach to ultrastrong and tough biomimic composites, Sci. Rep. 3 (2013) 1–8, https://doi.org/10.1038/srep02374.
[13] R. Mezzenga, J.M. Seddon, C.J. Drummond, B.J. Boyd, G.E. Schröder-Turk, L. Sagalowicz, Nature-inspired design and application of lipidic lyotropic liquid crystals, Adv. Mater. 31 (2019) 1–19, https://doi.org/10.1002/adma.201900818.
[14] X. Zhang, J. Liu, P. Cai, C. Kärnfelt, X. Wang, S. Ma, J. Morris, H. Zirath, Millimeter-wave ultra-wideband bandpass filter based on liquid crystal polymer substrates for automotive radar systems, Microw. Opt. Technol. Lett. 50 (2008) 2276–2280, https://doi.org/10.1002/mop.
[15] C. Song, R. Lan, C. Shen, J. Bao, R. Huang, Z. Wang, L. Zhang, M. Yu, S. Zhu, Self-adaptive accommodative intraocular lens enabled by sunlight-driven highly transparent liquid crystalline polymers, ACS Appl. Polym. Mater. (2022), https://doi.org/10.1021/acsapm.2c00091.
[16] Z. Zhang, X. Yang, Y. Zhao, F. Ye, L. Shang, Liquid crystal materials for biomedical applications, Adv. Mater. 35 (2023) 1–29, https://doi.org/10.1002/adma.202300220.
[17] M.A. Hussein, M.A. Abdel-Rahman, A.M. Asiri, K.A. Alamry, K.I. Aly, Review on: liquid crystalline polyazomethines polymers. Basics, syntheses and characterization, Des. Monomers Polym. 15 (2012) 431–463, https://doi.org/10.1080/1385772X.2012.688325.
[18] H. Finkelmann, H.J. Kock, G. Rehage, Phase studies of liquid crystalline side chain polymers mixed with low molar mass liquid crystals of similar structure, Mol. Cryst. Liq. Cryst. 89 (1982) 23–36, https://doi.org/10.1080/00268948208074466.
[19] H.J. Sun, S. Zhang, V. Percec, From structure to function via complex supramolecular dendrimer systems, Chem. Soc. Rev. 44 (2015) 3900–3923, https://doi.org/10.1039/c4cs00249k.
[20] J.C. Ronda, J.A. Reina, M. Giamberini, Self-organized liquid-crystalline polyethers obtained by grafting tapered mesogenic groups onto poly(epichlorohydrin): toward biomimetic ion channels 2, J. Polym. Sci. Part A Polym. Chem. 42 (2004) 326–340, https://doi.org/10.1002/pola.11016.
[21] S.V. Bhosale, M.A. Rasool, J.A. Reina, M. Giamberini, New liquid crystalline columnar poly(epichlorohydrin-co-ethylene oxide) derivatives leading to biomimetic ion channels, Polym. Eng. Sci. 53 (2013) 159–167, https://doi.org/10.1002/pen.
[22] X. Montané, S.V. Bhosale, J.A. Reina, M. Giamberini, Columnar liquid crystalline polyglycidol derivatives: a novel alternative for proton-conducting membranes, Polymer 66 (2015) 100–109, https://doi.org/10.1016/j.polymer.2015.03.071.
[23] A. Šakalyte, J.A. Reina, M. Giamberini, Liquid crystalline polyamines containing side dendrons: toward the building of ion channels based on polyamines, Polymer 54 (2013) 5133–5140, https://doi.org/10.1016/j.polymer.2013.07.027.
[24] X. Montané, K.A. Bogdanowicz, G. Colace, J.A. Reina, P. Cerruti, A. Lederer, M. Giamberini, Advances in the design of self-supported ion-conducting membranes-new family of columnar liquid crystalline polyamines. Part 1: copolymer synthesis and membrane preparation, Polymer 105 (2016) 298–309, https://doi.org/10.1016/j.polymer.2016.10.047.
[25] V. Percec, J. Heck, Liquid crystalline polymers containing mesogenic units based on half-disc and rod-like moieties. 1. Synthesis and characterization of 4-(11-Undecan-1-yloxy)-4'-[3,4,5-Tri(p-n-Dodecan-1-yloxybenzyloxy)benzoate] biphenyl side groups, J. Polym. Sci. Part A Polym. Chem. 29 (1991) 591–597.
[26] J. Guardià, M. Giamberini, J.A. Reina, X. Montané, Synthesis and characterization of dendronized side chain liquid crystalline Poly(2-oxazoline)s towards biomimetic ion channels, Eur. Polym. J. 196 (2023), https://doi.org/10.1016/j.eurpolymj.2023.112273.
[27] B. Tylkowski, N. Castelao, M. Giamberini, R. Garcia-Valls, J.A. Reina, T. Gumí, The importance of orientation in proton transport of a polymer film based on an oriented self-organized columnar liquid-crystalline polyether, Mater. Sci. Eng. C 32 (2012) 105–111, https://doi.org/10.1016/j.msec.2011.10.003.
[28] X. Montané, K.A. Bogdanowicz, J. Prats-Reig, G. Colace, J.A. Reina, M. Giamberini, Advances in the design of self-supported ion-conducting membranes – new family of columnar liquid crystalline polyamines. Part 2: ion transport characterisation and comparison to hybrid membranes, Polymer 105 (2016) 234–242, https://doi.org/10.1016/j.polymer.2016.10.046.
[29] A. Rapp, I. Schnell, D. Sebastiani, S.P. Brown, V. Percec, H.W. Spiess, Supramolecular assembly of dendritic polymers elucidated by 1H and 13C solid-state MAS NMR spectroscopy, J. Am. Chem. Soc. 125 (2003) 13284–13297, https://doi.org/10.1021/ja035127d.
[30] M.R. Hansen, R. Graf, H.W. Spiess, Interplay of structure and dynamics in functional macromolecular and supramolecular systems as revealed by magnetic resonance spectroscopy, Chem. Rev. 116 (2016) 1272–1308, https://doi.org/10.1021/acs.chemrev.5b00258.
[31] M.N. Garaga, L. Murdock, T. Pranto, S. Suarez, B.C. Benicewicz, S.G. Greenbaum, NMR investigation of proton transport in polybenzimidazole/polyphosphoric acid membranes prepared via novel synthesis route, J. Power Sources 575 (2023) 233169, https://doi.org/10.1016/j.jpowsour.2023.233169.
[32] M. Tress, K. Xing, S. Ge, P. Cao, T. Saito, A. Sokolov, What dielectric spectroscopy can tell us about supramolecular networks, Eur. Phys. J. E. 42 (2019), https://doi.org/10.1140/epje/i2019-11897-4.
[33] R. Teruel-Juanes, K.A. Bogdanowicz, J.D. Badia, V.S. de Juano-Arbona, R. Graf, J. A. Reina, M. Giamberini, A. Ribes-Greus, Molecular mobility in oriented and unoriented membranes based on poly[2-(Aziridin-1-yl)ethanol], Polymers 13 (2021) 1060, https://doi.org/10.3390/polym13071060.
[34] R. Teruel-Juanes, B. Pascual-Jose, R. Graf, J.A. Reina, M. Giamberini, A. Ribes-Greus, Effect of dendritic side groups on the mobility of modified poly (epichlorohydrin) copolymers, Polymers 13 (2021) 1961.
[35] B. Pascual-Jose, A. Zare, S. De la Flor, J.A. Reina, M. Giamberini, A. Ribes-Greus, Dielectric properties in oriented and unoriented membranes based on poly (epichlorohydrin-co-ethylene oxide) copolymers: Part III, Polymers 14 (2022), https://doi.org/10.3390/polym14071369.
[36] A. Šakalyte, J.A. Reina, M. Giamberini, A. Lederer, Preparation of a versatile precursor of novel functionalized polymers: the influence of polymerization conditions on the structure of poly [1-(2-hydroxyethyl)aziridine], Polym. Eng. Sci. 54 (2014) 579–591, https://doi.org/10.1002/pen.23590.